

# Geophysical Research Letters<sup>®</sup>



## RESEARCH LETTER

10.1029/2023GL104452

## On the Genesis of the 2021 Atlantic Niño

Sang-Ki Lee<sup>1</sup> , Hosmay Lopez<sup>1</sup> , Franz Philip Tuchen<sup>1</sup> , Dongmin Kim<sup>1,2</sup> , Gregory R. Foltz<sup>1</sup> , and Andrew T. Wittenberg<sup>3</sup> 

<sup>1</sup>Atlantic Oceanographic and Meteorological Laboratory, NOAA, Miami, FL, USA, <sup>2</sup>Cooperative Institute for Marine and Atmospheric Studies, University of Miami, Miami, FL, USA, <sup>3</sup>Geophysical Fluid Dynamics Laboratory, NOAA, Princeton, NJ, USA

### Key Points:

- The extreme 2021 Atlantic Niño was preconditioned by a series of oceanic Rossby waves reflected into downwelling equatorial Kelvin waves
- One of the Kelvin waves was greatly amplified by an intense week-long westerly wind burst event, initiating the 2021 Atlantic Niño
- The westerly wind burst was driven by the Madden-Julian Oscillation, which is a previously unidentified driver for Atlantic Niño

### Supporting Information:

Supporting Information may be found in the online version of this article.

### Correspondence to:

S.-K. Lee,  
Sang-Ki.Lee@noaa.gov

### Citation:

Lee, S.-K., Lopez, H., Tuchen, F. P., Kim, D., Foltz, G. R., & Wittenberg, A. T. (2023). On the genesis of the 2021 Atlantic Niño. *Geophysical Research Letters*, 50, e2023GL104452. <https://doi.org/10.1029/2023GL104452>

Received 5 MAY 2023  
Accepted 11 AUG 2023

### Author Contributions:

**Conceptualization:** Sang-Ki Lee, Hosmay Lopez  
**Formal analysis:** Sang-Ki Lee, Hosmay Lopez, Franz Philip Tuchen  
**Investigation:** Sang-Ki Lee, Hosmay Lopez, Franz Philip Tuchen, Dongmin Kim, Gregory R. Foltz  
**Methodology:** Sang-Ki Lee, Hosmay Lopez, Franz Philip Tuchen  
**Writing – original draft:** Sang-Ki Lee

Published 2023. This article is a U.S. Government work and is in the public domain in the USA.

This is an open access article under the terms of the [Creative Commons Attribution-NonCommercial License](https://creativecommons.org/licenses/by/4.0/), which permits use, distribution and reproduction in any medium, provided the original work is properly cited and is not used for commercial purposes.

**Abstract** An extreme Atlantic Niño developed in the boreal summer of 2021 with peak-season sea surface temperature anomalies exceeding 1°C in the eastern equatorial region for the first time since global satellite measurements began in the early 1970s. Here, we show that the development of this outlier event was preconditioned by a series of oceanic Rossby waves that reflected at the South American coast into downwelling equatorial Kelvin waves. In early May, an intense week-long westerly wind burst (WWB) event, driven by the Madden-Julian Oscillation (MJO), developed in the western and central equatorial Atlantic and greatly amplified one of the reflected Kelvin waves, directly initiating the 2021 Atlantic Niño. MJO-driven WWBs are fundamental to the development of El Niño in the Pacific but are a previously unidentified driver for Atlantic Niño. Their importance for the 2021 event suggests that they may serve as a useful predictor/precursor for future Atlantic Niño events.

**Plain Language Summary** Atlantic Niño is the Atlantic counterpart of El Niño in the Pacific, often referred to as El Niño's little brother. It was previously thought to have only regional influence on rainfall variability in West Africa, but a growing number of studies have shown that Atlantic Niño also plays an important role in the development of El Niño–Southern Oscillation, as well as in the formation of powerful hurricanes near the coast of West Africa. This study investigates the development of an extreme Atlantic Niño in the summer of 2021. Here, we show that the 2021 event was preconditioned by warm waters piled up near the South American coast, and then directly triggered by a westerly wind burst event that drove the warm waters eastward. The westerly wind burst event was driven by a patch of tropical thunderstorms that formed across the Indian Ocean and moved slowly eastward across the Pacific, South America, and the Atlantic, also known as the Madden-Julian Oscillation. Westerly wind bursts driven by the Madden-Julian Oscillation are fundamental for the development of El Niño in the Pacific, but a previously unidentified driver for Atlantic Niño, and thus may improve our ability to predict future Atlantic Niño events.

## 1. Introduction

In the boreal summer of 2021, the eastern equatorial Atlantic Ocean had record-high sea surface temperature anomalies (SSTAs), producing the most extreme Atlantic Niño event recorded since global satellite measurements began in the early 1970s (Figures 1a–1c). Heavy rainfall and multiple flooding events were reported in the West African countries bordering the Gulf of Guinea (Figure 1d; Bissolli et al., 2022) in agreement with the causal relationship between warm eastern equatorial Atlantic SSTAs and an enhanced Atlantic intertropical convergence zone (ITCZ) rainband (e.g., Carton & Huang, 1994; Folland et al., 2001; Foltz et al., 2019; Giannini, 2003; Losada et al., 2010; Lübbecke et al., 2018; Okumura & Xie, 2004; Tschakert et al., 2010; Vallès-Casanova et al., 2020). A recent study showed that the enhanced ITCZ during Atlantic Niño promotes the development of deep tropical hurricanes off the coast of West Africa (Kim et al., 2023); this suggests that the 2021 Atlantic Niño may also have contributed to the highly active hurricane season of that year. As such, the 2021 Atlantic Niño presents a rare opportunity to improve our understanding of the ocean and atmosphere processes involved in the development of extreme Atlantic Niño conditions.

Earlier studies have shown that historical Atlantic Niño events were often triggered by external forcings, such as the El Niño–Southern Oscillation (ENSO) and the Atlantic Meridional Mode (AMM) (e.g., Carton & Huang, 1994; Chang et al., 2006; Foltz & McPhaden, 2010; Jiang et al., 2022; Keenlyside & Latif, 2007; Latif & Grötzner, 2000; Lübbecke & McPhaden, 2012; Martín-Rey et al., 2018; Martín-Rey & Lazar, 2019; Tokinaga et al., 2019; Vallès-Casanova et al., 2020). Indeed, the 2021 Atlantic Niño occurred between two consecutive

**Writing – review & editing:** Sang-Ki Lee, Hosmay Lopez, Franz Philip Tuchen, Dongmin Kim, Gregory R. Foltz, Andrew T. Wittenberg

La Niña events of 2020–2021 and 2021–2022. However, the 2021 Atlantic Niño is a clear outlier, with its peak-season (June–August) SSTAs exceeding 1°C in the eastern equatorial region (20°W–0°, 3°S–3°N; ATL3) for the first time since the early 1970s (Figure 1a); thus, previously identified mechanisms may not explain the development of the extreme 2021 event. Therefore, to address what caused the development of the 2021 Atlantic Niño, it may be helpful to look into earlier works on the genesis of the most intense El Niño events in the Pacific, given that Atlantic Niño can be considered the Atlantic counterpart of El Niño (e.g., Keenlyside & Latif, 2007; Latif et al., 1996; Latif & Grötzner, 2000; Philander, 1986; Zebiak, 1993).

It is well established that El Niño is largely preconditioned by a slow buildup of upper ocean heat in the western Pacific warm pool region (e.g., Jin, 1997; Meinen & McPhaden, 2000; Suarez & Schopf, 1988; Wyrski, 1985). While external forcing is generally not required to initiate El Niño, stochastic forcing has been shown to be central to El Niño onset, growth, and irregularity, as well as ENSO phase asymmetry (e.g., Chang et al., 1996; Kirtman & Schopf, 1998; Lopez & Kirtman, 2015; Penland & Sardeshmukh, 1995; Timmermann et al., 2018). This stochastic forcing consists mainly of episodic westerly wind bursts (WWBs) in the western equatorial Pacific, which are often linked to the convectively-active phase of the Madden-Julian Oscillation (MJO) (e.g., Chiodi et al., 2014; Kessler, 2002; McPhaden, 1999, 2004; Puy et al., 2016). A sufficiently intense season of WWBs can drive an equatorial oceanic downwelling Kelvin wave train that can initiate El Niño (e.g., Kessler et al., 1995; Luther et al., 1983; McPhaden, 1999, 2004; McPhaden et al., 1988) and amplify its growth (e.g., Hu & Fedorov, 2019; Lengaigne et al., 2004; Vecchi & Harrison, 2000). In particular, the most intense El Niño events (such as in 1997–1998) appear to require both sufficient ocean preconditioning and sustained WWB activity (e.g., Kessler, 2002; McPhaden, 1999, 2004; Puy et al., 2019; van Oldenborgh, 2000; Vecchi et al., 2006). Therefore, it is reasonable to pose the question of whether WWBs were involved in the genesis of the 2021 Atlantic Niño.

The main goal of this study is to address local and remote ocean-atmosphere processes that led to the development of the 2021 Atlantic Niño. We first investigate whether WWBs linked to the MJO played a role in the onset of the 2021 event. We then explore preconditions of the event and their potential drivers, as well as the role of the preceding 2020–2021 La Niña. These questions are addressed through analysis of observations and atmosphere-ocean reanalysis products.

## 2. Data and Methods

To explore the development of the 2021 Atlantic Niño, we analyze several daily and monthly observational and reanalysis datasets. Monthly SSTs are derived from the Hadley Centre Sea Ice and SST data set version-1 (HadISST1, Rayner et al., 2003). A separate 30-year averaged climatology is constructed every 5 years and used to derive monthly SSTAs. Historical Atlantic Niño events during 1948–2021 are identified based on the threshold that the 3-month averaged SSTAs exceed 0.5°C in the ATL3 region for at least two consecutive overlapping seasons. The AMM index is computed as the difference in SSTAs between the tropical North Atlantic (50°–20°W, 5°–15°N) and tropical South Atlantic (20°W–10°E, 15°–5°S). The upper and lower terciles are used to define the positive (+) and negative (–) AMM.

Monthly precipitation anomalies are derived from the National Oceanic and Atmospheric Administration (NOAA)'s gauge observation-based global land precipitation reconstruction (Chen et al., 2002). Monthly anomalies of surface winds (at 10 m) are from the National Centers for Environmental Prediction-National Center for Atmospheric Research reanalysis (NCEP reanalysis, Kalnay et al., 1996). Daily anomalies of zonal winds at 10 m, 850 hPa, and 200 hPa are also from the NCEP reanalysis. Daily anomalies of equatorial Atlantic surface zonal winds derived from the NCEP reanalysis are compared with those from the European Center for Medium-Range Weather Forecasts (ECMWF) reanalysis-5 (ERA5, Hersbach et al., 2020) and Prediction and Research Moored Array in the Tropical Atlantic (PIRATA, Boulès et al., 2019) mooring stations along the equator. Daily outgoing long-wave radiation (OLR) anomalies are from NOAA's interpolated gridded data set (Liebmann & Smith, 1996).

Daily sea surface height (SSH) anomalies, which are used here as proxies for thermocline depth anomalies for the period of 1993–2021, are from the Archiving, Validation, and Interpretation of Satellite Oceanographic data (AVISO). Monthly SSH anomalies derived from ECMWF Ocean Reanalysis System 5 (Zuo et al., 2017) for the period of 1958–1992 are merged with monthly SSH anomalies derived from AVISO for the later period of 1993–2021. To focus on dynamic variability, the linear trends in global mean SSH in the two datasets are subtracted before merging the two datasets.

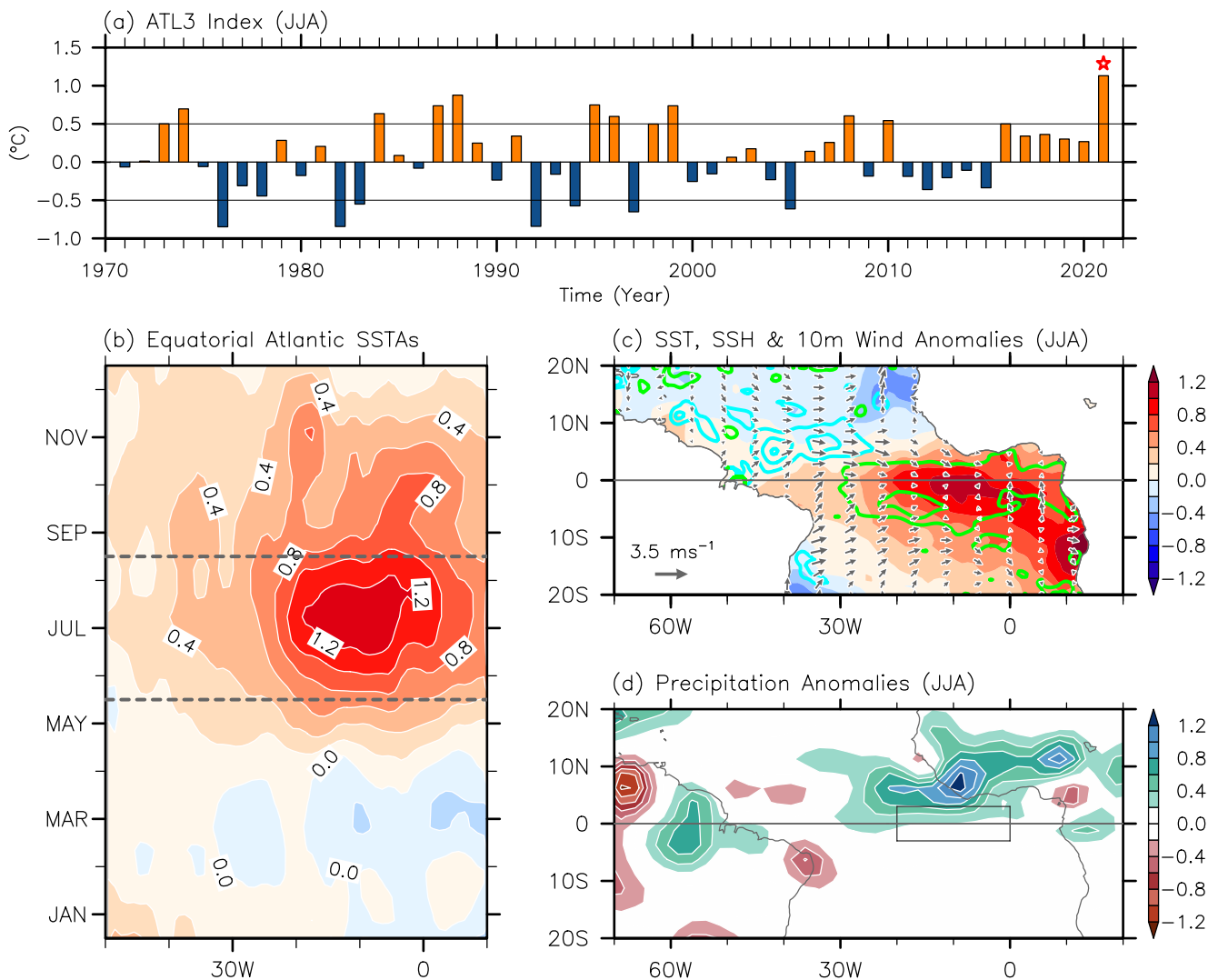


**Figure 1.** (a) Time series of June–August averaged SSTAs in the eastern equatorial region (20°W–0°, 3°S–3°N; ATL3). (b) Time-longitude plot of equatorial Atlantic SSTAs, averaged between 3°S and 3°N, from January to December 2021. (c) Tropical Atlantic SST (shades), SSH (contours) and 10-m wind (vectors) anomalies, and (d) precipitation anomalies during June–August 2021. Positive and negative SSHAs are indicated by green and cyan contour lines, respectively in (c). The ATL3 region is indicated in (d). The units for SST, SSH, 10-m wind, and precipitation are in °C, cm, m s<sup>-1</sup>, and mm day<sup>-1</sup>, respectively. The contour interval for SSH anomalies is 2.0 cm.

The Real-time Multivariate MJO (RMM) indices (Wheeler & Hendon, 2004) are computed based on the daily zonal wind anomalies at 850 and 200 hPa, and daily OLR anomalies. A subseasonal filter (20–100-day band-pass) was applied prior to computing the MJO indices. The time series of the first and second empirical orthogonal functions, namely RMM1 and RMM2, can be used to produce an MJO phase diagram (Figure S1 in Supporting Information S1). Based on the combination of RMM1 and RMM2 values, an MJO phase diagram can be divided into eight sectors, with each sector indicating different phases of MJO propagation toward the east. The eastward propagation of MJO can be traced by a trajectory of anti-clockwise circles in the MJO phase diagram. Figure S2 in Supporting Information S1 describes the observed MJO cycle during each of the eight phases.

### 3. MJO-Driven Onset of the 2021 Atlantic Niño

Figure 2a shows daily SSH anomalies along the equatorial Atlantic (3°S–3°N) for the period of 1 January–1 September 2021. It shows a slow buildup of upper ocean heat in the western basin in the winter and spring of 2021. But, more importantly, it clearly shows that the 2021 warm event was triggered by an intense downwelling Kelvin wave that originated from the South American coast between mid-April and early May and was forced in

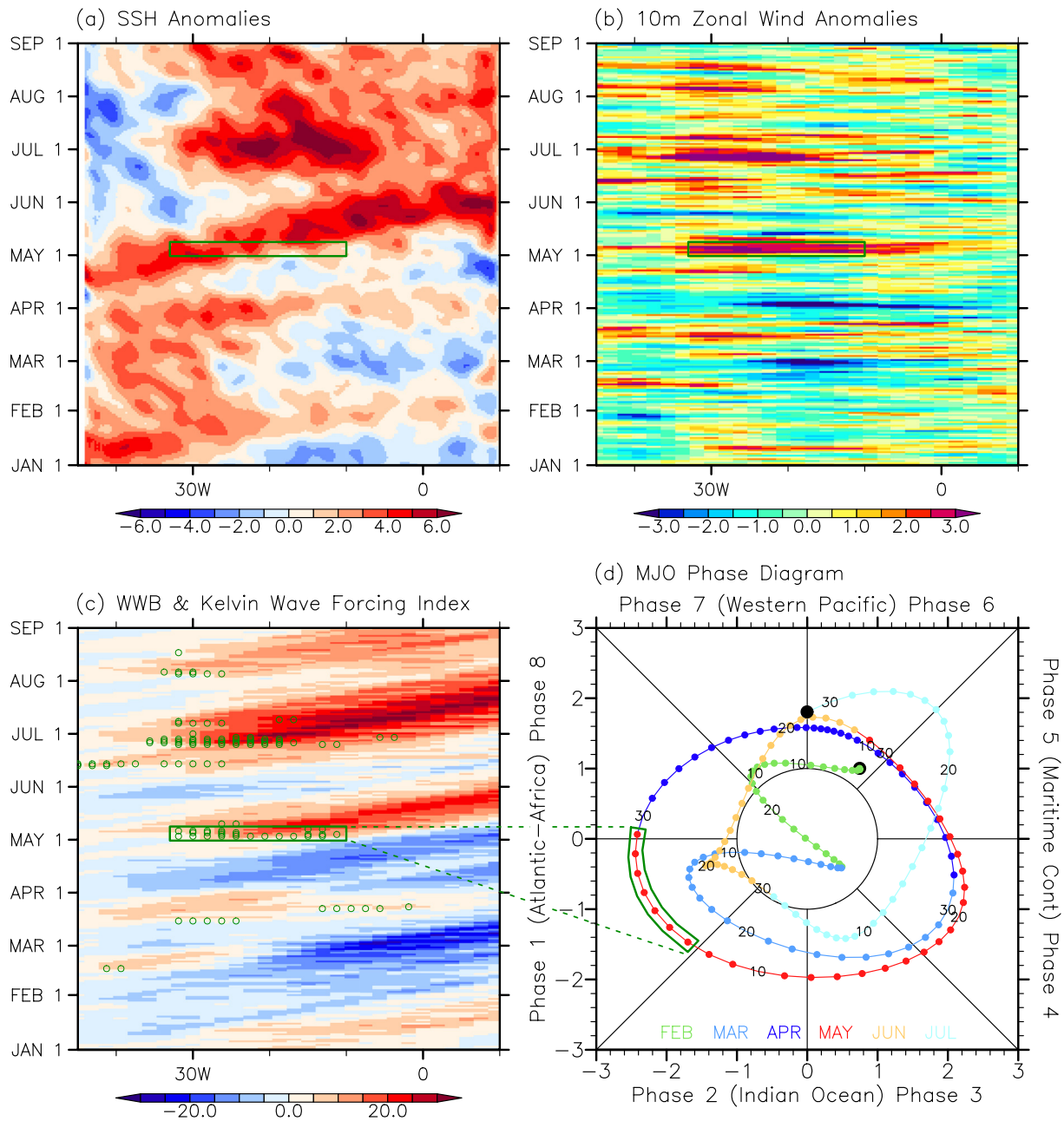


**Figure 2.** (a–c) Time-longitude plots of equatorial Atlantic (a) SSH anomalies (in cm), (b) 10-m zonal wind anomalies (in  $\text{m s}^{-1}$ ), and (c) Kelvin wave forcing index ( $K$ , in  $\text{m}^2 \text{s}^{-1}$ ) during 1 January–1 September 2021. (d) MJO phase diagram for the period of 1 February–31 July 2021. The green boxes in (a), (b) and (c) indicate the zonal extent ( $33^{\circ}\text{W}$ – $10^{\circ}\text{W}$ ) and the timing (1–7 May 2021) of a strong WWB event. Green circles in (c) indicate daily zonal wind anomalies greater than  $3 \text{ m s}^{-1}$ . The phase-1 MJO event during the first seven days of May 2021 is highlighted by a green polygon in (d). The two dashed lines in between (c) and (d) indicate 1 and 7 May 2021.

part by a reflected Rossby wave (discussed in Section 4). The corresponding daily zonal wind anomalies along the equatorial Atlantic (Figure 2b) suggest that the downwelling Kelvin wave was also forced by a strong WWB event in the western and central basin ( $33^{\circ}\text{W}$ – $10^{\circ}\text{W}$ ) during the first seven days of May 2021. This week-long WWB event was strong enough to reverse the climatological easterly winds and produce net westerly flow in the region (Figure S3 in Supporting Information S1), and is also well captured by a PIRATA mooring at  $23^{\circ}\text{W}$  in the central equatorial Atlantic and in ERA5 (Figure S4 in Supporting Information S1).

As discussed by Kessler et al. (1995), the Kelvin wave response to equatorial zonal wind anomalies is proportional to the wind anomalies integrated over the patch along the Kelvin wave characteristic lines. Therefore, it can

be measured by a Kelvin wave forcing index ( $K$ , Zhang & Gottschalck, 2002) at a given longitude  $x_0$  and time  $t_0$ , which can be written as

$$K(x_0, t_0) = \int_0^x U_{10} \left( x, t_0 - \frac{x_0 - x}{c} \right) dx, \quad (1)$$

where  $x = 0$  is the longitude of the western boundary,  $U_{10}$  is equatorial zonal wind anomalies, and  $c = 1.8 \text{ m s}^{-1}$  is the observed Kelvin wave phase speed in the equatorial Atlantic (e.g., Polo et al., 2008). Figure 2c confirms that during the first 7 days of May 2021, the WWB event, defined here as daily zonal wind anomalies greater than  $3 \text{ m s}^{-1}$  (indicated by green circles), directly forced the downwelling Kelvin wave that initiated the 2021 Atlantic Niño.

The WWB event persisted for a week in the western and central basin (Figure 2b); thus, it cannot be explained by locally generated convectively coupled atmospheric Kelvin waves that propagate eastward rather quickly, typically crossing the Atlantic basin in 2–4 days (e.g., Wang & Fu, 2007; Zhao & Fu, 2022). As shown in the MJO phase diagram for the period of 1 February–31 July 2021 (Figure 2d), a strong phase-1 MJO event persisted during the first seven days of May 2021, suggesting that the WWB event during that period is linked to this phase-1 MJO event. Figure 2d and Figure S5 in Supporting Information S1 also show that this MJO event first developed in the Indian Ocean in late March, and then propagated eastward to the Pacific and the Atlantic, leading up to the WWB event in early May. To further explore the causality between the WWB event and the phase-1 MJO during 1–7 May 2021, all MJO events that occurred during 1982–2021 (200–300 events for each phase) are assembled, and their westerly wind anomalies greater than  $3 \text{ m s}^{-1}$  are used to compute  $K$  for each of the eight MJO phases. As shown in Figure 3a, downwelling Kelvin waves, forced by WWB events, are generated predominantly during MJO phase-1 and then propagate eastward during the following MJO phases 2–5.

Furthermore, strong low-level westerly wind anomalies and negative OLR anomalies (i.e., increased convection) that prevailed along the equatorial Atlantic during 1–7 May 2021 (Figure 3b) are largely consistent with those from the composite of all phase-1 MJO events (Figure 3c). Figure 3d further shows suppressed convection (i.e., positive OLR anomalies) over the western Pacific and increased convection (negative OLR anomalies) in the Atlantic Ocean, Africa, and the western Indian Ocean during 1–7 May 2021. These signals are directly related to low-level westerly wind anomalies in the Pacific and Atlantic Oceans and easterly anomalies over the Indian Ocean. These patterns of OLR and zonal wind anomalies are also largely in agreement with those from the composite map of historical phase-1 MJO events (Figure 3e). Nevertheless, while the composite zonal wind anomalies are stronger north of the equator and weaker along the equator (e.g., Matthews, 2000; Yu et al., 2011), the equatorial zonal wind anomalies during the first week of May 2021 were disproportionately stronger.

For several days prior to and after 20 June 2021, a secondary WWB event occurred in response to another phase-1 MJO event (Figures 2b and 2d and Figure S5 in Supporting Information S1). As a result, the equatorial thermocline deepened greatly from late June to early July; this suggests that the second WWB event reinforced the 2021 Atlantic Niño (Figures 2a and 2c). Therefore, it appears that the 2021 Atlantic Niño was both initiated and reinforced by two separate phase-1 MJO events and associated WWBs.

#### 4. Rossby Wave Reflection and Generation of Equatorial Kelvin Wave

As shown in the previous section, the 2021 Atlantic Niño was initiated by a strong downwelling equatorial Kelvin wave, which was forced in part by a week-long WWB event associated with a phase-1 MJO event. However, comparing the observed SSH anomalies and Kelvin wave forcing index ( $K$ ) (Figures 2a and 2c), it appears that the generation of the downwelling Kelvin wave off the South American coast and its initial propagation to around  $33^\circ\text{W}$  were not directly forced by the WWB event. Previous studies have shown that downwelling Kelvin waves in the equatorial Atlantic are often generated when Rossby waves originating north of the equator are reflected at the South American coast (e.g., Foltz & McPhaden, 2010; Martín-Rey & Lazar, 2019; Richter et al., 2022). Indeed, as shown in Figure 4a, Figure S6 and S7a in Supporting Information S1, a series of Rossby waves with deeper than normal thermocline in the latitude band of  $3^\circ\text{--}6^\circ\text{N}$  formed west of around  $20^\circ\text{W}$  after 1 January 2021, and then propagated toward the South American coast at a speed of around  $0.4 \text{ m s}^{-1}$ , which is consistent with the observed range of  $0.35\text{--}0.4 \text{ m s}^{-1}$  (e.g., Schouten et al., 2005). These downwelling equatorial Rossby waves

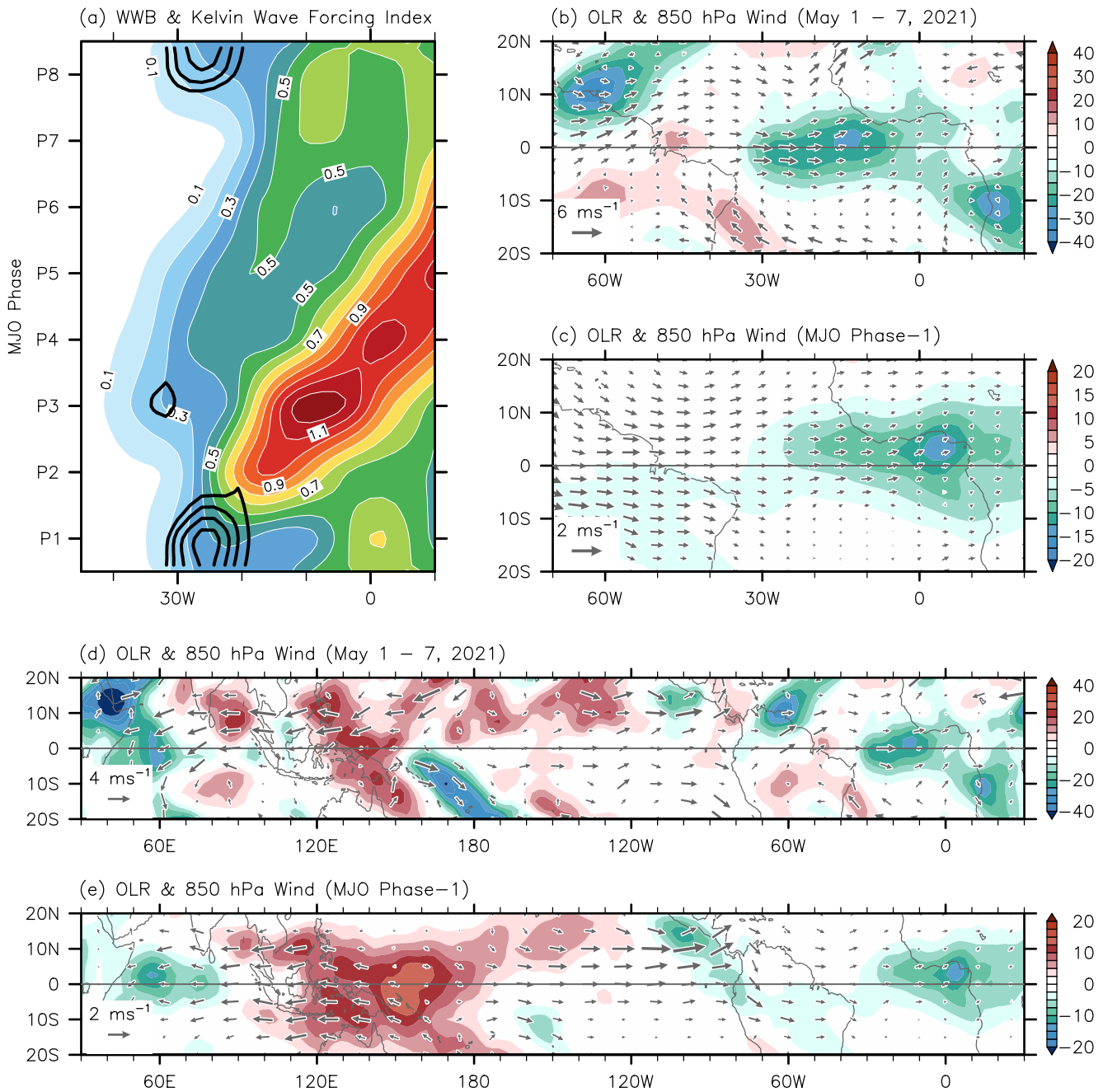


**Figure 3.** (a) Kelvin wave forcing index ( $K$ , shaded) and WWBs (contours) for each of the eight MJO phases derived from all MJO events that occurred during 1982–2021. For each of the eight MJO phases, around 200–300 events are selected, and their westerly wind anomalies greater than  $3 \text{ m s}^{-1}$  are used to compute  $K$ , which is then averaged by the number of all MJO events. Low-level (850 hPa) wind and OLR anomalies during (b) 1–7 May 2021, and from (c) all phase-1 MJO events during 1982–2021. Panels (d) and (e) are the same as (b) and (c), respectively, but for the global tropical region. The units for  $K$ , WWBs, low-level wind, and OLR are in  $\text{m}^2 \text{ s}^{-1}$ ,  $\text{m s}^{-1}$ ,  $\text{m s}^{-1}$ , and  $\text{W m}^{-2}$ , respectively. The contour levels for WWBs in (a) are from  $0.07$  to  $0.1 \text{ m s}^{-1}$ , with an interval of  $0.01 \text{ m s}^{-1}$ .

appear to be initiated by Ekman convergence driven by westerly wind anomalies and associated negative wind curl anomalies that persisted throughout January–March 2021, as shown in Figures S6 and S7b in Supporting Information S1 and also indicated by purple circles in Figure 4a.

About three downwelling Kelvin waves were generated as the Rossby waves reflected from the South American coast during the winter and spring of 2021 (Figure 4b). Two of those, one during early-to-mid January and the other during mid-to-late March, propagated eastward along the equatorial Atlantic. However, without help from

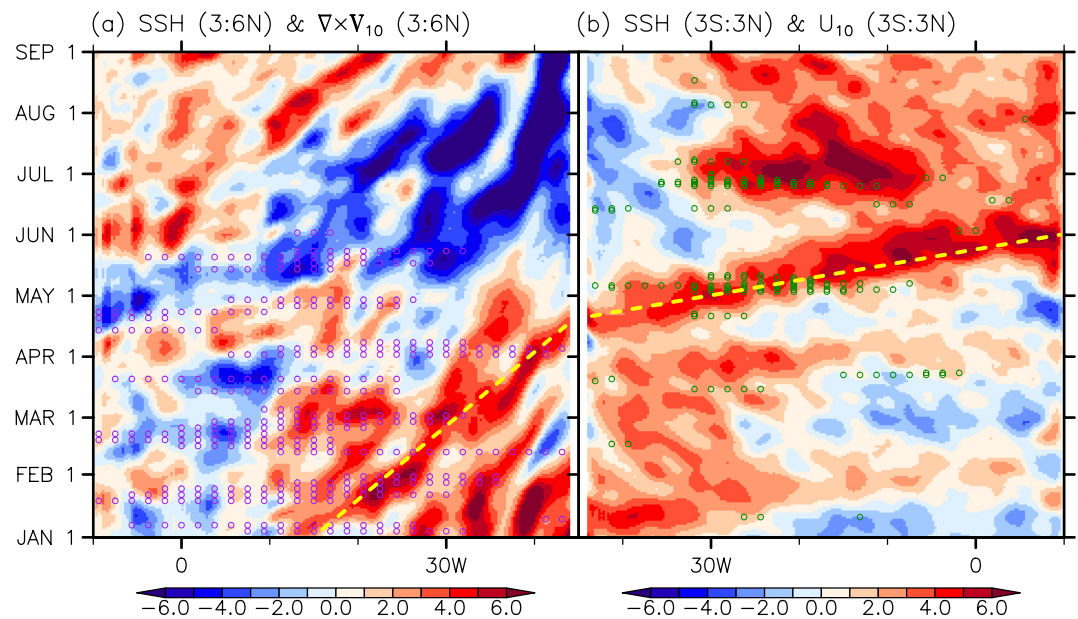


**Figure 4.** Time-longitude plots of SSH anomalies (a) in the latitude band of  $3^{\circ}$ – $6^{\circ}$ N, and (b) along the equatorial Atlantic ( $3^{\circ}$ S– $3^{\circ}$ N) from 1 January to 1 September 2021. Note that the longitude (x-axis) in (a) is reversed for better visual comparison with downwelling Kelvin waves shown in (b). Purple circles in (a) indicate daily 10-m wind curl anomalies in the latitude band of  $3^{\circ}$ – $6^{\circ}$ N less than  $-0.6 \times 10^{-6} \text{ s}^{-1}$  from 1 January to 1 June 2021 (shown for every three days). Similarly, green circles in (b) indicate daily 10-m zonal wind anomalies along the equator ( $3^{\circ}$ S– $3^{\circ}$ N) greater than  $3 \text{ m s}^{-1}$  from 1 January to 1 September 2021. The yellow dashed lines in (a) and (b) are based on the estimated values of Rossby wave speed ( $0.4 \text{ m s}^{-1}$ ) and Kelvin wave speed ( $1.8 \text{ m s}^{-1}$ ), respectively. The unit for SSH anomalies is cm.

WWBs, they dissipated before reaching the West African coast. Only one reflected Kelvin wave that was generated around mid-to-late April further developed into a full-scale downwelling Kelvin wave and reached the West African coast due to the MJO-driven WWB event during 1–7 May 2021 (Figure 2).

## 5. Discussion

### 5.1. Did the 2020–2021 La Niña Play a Role?

Among the 22 historical Atlantic Niño events that occurred during 1948–2020, six of them followed the winter peak of La Niña, while nine followed the winter peak of El Niño and seven followed ENSO-neutral winter (Figure S8j and Table S1 in Supporting Information S1). La Niña, via extratropical atmospheric pathways, tends to increase the trade winds in the tropical North Atlantic in winter and produces a negative phase of the AMM in spring (Figures S8d–S8f in Supporting Information S1, e.g., Enfield & Mayer, 1997; Alexander & Scott, 2002; Lee et al., 2008). The (–) AMM in turn produces equatorial westerly wind anomalies; thus, the zonal thermocline slope is relaxed along the equator, forcing Atlantic Niño (e.g., Vallès-Casanova et al., 2020). Indeed, all six Atlantic Niño events that followed the winter peak of La Niña were driven by the above mechanism involving the formation of (–) AMM (Table S1 in Supporting Information S1).

However, the seasonal evolutions of SST, surface wind, and SSH anomalies in the winter and spring prior to the 2021 Atlantic Niño (Figures S8a–S8c in Supporting Information S1) look very different from those in the La Niña composites (Figures S8d–S8f in Supporting Information S1). They are also inconsistent with equatorial westerly wind anomalies (through regional Walker circulation anomalies) observed during some multi-year La Niña events (Tokinaga et al., 2019). Therefore, it is unlikely that the 2020–2021 La Niña had a significant influence on the onset of the 2021 Atlantic Niño, at least not in the canonical pathways that involve the formation of (–) AMM or regional Walker circulation anomalies in the preceding winter and spring.

### 5.2. What Caused the Off-Equatorial Westerly Wind Anomalies?

It should be noted that the 2020–2021 winter was a very unusual La Niña winter, partly due to the development of sudden stratospheric warming that led to a disruption of the stratospheric polar vortex (Dunn et al., 2022; Lu

et al., 2021). As such, it is hard to attribute the large-scale atmospheric patterns in the winter and spring of 2021 to any particular climate signals. Nevertheless, it is interesting to note that tropical Atlantic SSTAs in the winter of 2020–2021 have a distinctive interhemispheric structure similar to the positive phase of the AMM (Figure S8a in Supporting Information S1).

Seven of the 22 historical Atlantic Niño events followed the spring or winter peak of (+) AMM, while 13 followed the spring or winter peak of (–) AMM, and only two followed AMM-neutral spring or winter (Figure S8k in Supporting Information S1). The (+) AMM develops in conjunction with a decrease in the trade winds in the tropical North Atlantic (Figures S8g–S8i in Supporting Information S1, e.g., Chiang & Vimont, 2004). As summarized in Foltz and McPhaden (2010) and others, the associated Ekman convergence produces a deeper-than-normal thermocline equatorward of the reduced trade winds. The deepened thermocline anomalies propagate westward as a Rossby wave and then reflect from the South American coast to initiate a downwelling equatorial Kelvin wave, thus triggering Atlantic Niño. Therefore, the (+) AMM-like SSTAs that appeared in the winter of 2020–2021 are potentially linked to the persistent westerly wind anomalies in the tropical North Atlantic and the associated negative wind curl anomalies during January–March of 2021 (Figure 4a, Figures S6 and S7b in Supporting Information S1).

## 6. Concluding Remarks

Using observations and reanalysis datasets, we show that the MJO and associated WWBs played a key role in initiating the 2021 Atlantic Niño. The 2021 event was preconditioned by a series of downwelling oceanic Rossby waves forced by persistent westerly wind anomalies in the latitude band of 6°–9°N throughout the winter and spring of 2021. These oceanic Rossby waves propagated westward and then reflected from the South American coast to generate several downwelling Kelvin waves along the equatorial Atlantic. One of the Kelvin waves that formed in mid-to-late April was greatly amplified by an MJO-driven WWB event on 1–7 May 2021, and directly forced the 2021 Atlantic Niño. Additionally, a secondary MJO-driven WWB event occurred for several days prior to and after 20 June 2021, further deepening the equatorial thermocline, and thus potentially reinforcing the 2021 Atlantic Niño. An interhemispheric pattern of tropical Atlantic SSTAs similar to (+) AMM appeared in the winter of 2020–2021, and potentially played a role in generating the off-equatorial westerly wind anomalies that persisted during January–March of 2021 and preconditioned the 2021 Atlantic Niño. We find no clear evidence that the 2020–2021 La Niña played a role in either preconditioning or directly forcing the 2021 Atlantic Niño, at least not in the canonical inter-basin pathways that involve the formation of (–) AMM or regional Walker circulation anomalies.

There are many remaining questions. Perhaps, the most important one is why this particular MJO event led to the most extreme Atlantic Niño given that multiple MJO events occur every year. Several factors may be at play. First, this phase-1 MJO event in the first week of May 2021 was very strong (i.e.,  $>2 \times$  standard deviation). In particular, the associated WWB event was strong enough to reverse the climatological easterly winds and produce net westerly flow in the western and central equatorial Atlantic. On top of that, the strong phase-1 MJO event occurred immediately after the initiation of a downwelling equatorial Kelvin wave off the South American coast in the season just prior to or during the development of the cold water tongue. Therefore, the chance to have these factors satisfied altogether must be very low. However, it is unclear whether the MJO-driven onset of the 2021 Atlantic Niño was an isolated event, or if similar events have occurred in the past. Therefore, future studies should explore historical Atlantic Niño events and the potential role of MJO-driven WWBs in their development.

## Data Availability Statement

All data used in this paper are publicly available to download. The HadISST1 data were provided by the UK Met Office at <https://www.metoffice.gov.uk/hadobs/hadisst>. The NCEP reanalysis, the NOAA gauge observation-based global land precipitation reconstruction data, and NOAA's interpolated daily OLR gridded data set were provided by NOAA's Physical Sciences Laboratory at <https://psl.noaa.gov/data/gridded>. Daily AVISO SSH anomalies and daily ERA5 surface zonal wind anomalies were provided by the Copernicus Climate Change Service at <https://cds.climate.copernicus.eu>. The ECMWF Ocean Reanalysis System 5 data set was also provided by the Copernicus Climate Change Service at <https://cds.climate.copernicus.eu>. Surface zonal wind anomalies from PIRATA mooring stations were provided by NOAA's Pacific Marine Environmental Laboratory at <https://www.pmel.noaa.gov/tao/drupal/disdel>.

**Acknowledgments**

The authors acknowledge two anonymous reviewers and Renellys Perez for helpful comments and suggestions. This work was supported by NOAA's Atlantic Oceanographic and Meteorological Laboratory, NOAA's Climate Program Office and Weather Program Office. F.P.T. was supported by a National Research Council Research Associateship Award. This research was carried out in part under the auspices of the Cooperative Institute for Marine and Atmospheric Studies, a cooperative institute of the University of Miami, and NOAA, cooperative agreement NA 200AR4320472.

**References**

Alexander, M., & Scott, J. (2002). The influence of ENSO on air-sea interaction in the Atlantic. *Geophysical Research Letters*, 29(14), 46-1–46-4. <https://doi.org/10.1029/2001GL014347>

Bissolli, P., Ganter, C., Mekonnen, A., Sánchez-Lugo, A., & Zhu, Z. (Eds.) (2022). Regional climates [in “State of the climate in 2021“]. *Bulletin of the American Meteorological Society* (Vol. 103(8), pp. S341–S453). [https://doi.org/10.1175/2022BAMSStateoftheClimate\\_Chapter7.1](https://doi.org/10.1175/2022BAMSStateoftheClimate_Chapter7.1)

Bourlès, B., Araujo, M., McPhaden, M. J., Brandt, P., Foltz, G. R., Lumpkin, R., et al. (2019). PIRATA: A sustained observing system for tropical Atlantic climate research and forecasting. *Earth and Space Science*, 6(4), 577–616. <https://doi.org/10.1029/2018EA000428>

Carton, J. A., & Huang, B. (1994). Warm events in the tropical Atlantic. *Journal of Physical Oceanography*, 24(5), 888–903. [https://doi.org/10.1175/1520-0485\(1994\)024<0888:weitta>2.0.co;2](https://doi.org/10.1175/1520-0485(1994)024<0888:weitta>2.0.co;2)

Chang, P., Fang, Y., Saravanan, R., Ji, L., & Seidel, H. (2006). The cause of the fragile relationship between the Pacific El Niño and the Atlantic Niño. *Nature*, 443(7109), 324–328. <https://doi.org/10.1038/nature05053>

Chang, P., Ji, L., Li, H., & Flügel, M. (1996). Chaotic dynamics versus stochastic processes in El Niño-Southern Oscillation in coupled ocean-atmosphere models. *Physica D: Nonlinear Phenomena*, 98(2–4), 301–320. [https://doi.org/10.1016/0167-2789\(96\)00116-9](https://doi.org/10.1016/0167-2789(96)00116-9)

Chen, M., Xie, P., Janowiak, J. E., & Arkin, P. A. (2002). Global land precipitation: A 50-yr monthly analysis based on gauge observations. *Journal of Hydrometeorology*, 3, 249–266. [https://doi.org/10.1175/1525-7541\(2002\)003<0249:glpaym>2.0.co;2](https://doi.org/10.1175/1525-7541(2002)003<0249:glpaym>2.0.co;2)

Chiang, J. C. H., & Vimont, D. J. (2004). Analogous Pacific and Atlantic meridional modes of tropical atmosphere–ocean variability. *Journal of Climate*, 17(21), 4143–4158. <https://doi.org/10.1175/JCLI4953.1>

Chiodi, A. M., Harrison, D. E., & Vecchi, G. A. (2014). Subseasonal atmospheric variability and El Niño waveguide warming: Observed effects of the Madden–Julian Oscillation and westerly wind events. *Journal of Climate*, 27(10), 3619–3642. <https://doi.org/10.1175/JCLI-D-13-00547.1>

Dunn, R. J. H., Aldred, F., Gobron, N., Miller, J. B., & Willett, K. M. (Eds.) (2022). Global climate [in “State of the climate in 2021“]. *Bulletin of the American Meteorological Society* (Vol. 103(8), S11–S142). <https://doi.org/10.1175/BAMS-D-22-0092.1>

Enfield, D. B., & Mayer, D. A. (1997). Tropical Atlantic sea surface temperature variability and its relation to El Niño–Southern Oscillation. *Journal of Geophysical Research*, 102(C1), 929–945. <https://doi.org/10.1029/96JC03296>

Folland, C. K., Colman, A. W., Rowell, D. P., & Davey, M. K. (2001). Predictability of Northeast Brazil rainfall and real-time forecast skill, 1987–98. *Journal of Climate*, 14(9), 1937–1958. [https://doi.org/10.1175/1520-0442\(2001\)014<1937:ponbra>2.0.co;2](https://doi.org/10.1175/1520-0442(2001)014<1937:ponbra>2.0.co;2)

Foltz, G., Brandt, P., Richter, I., Rodríguez-Fonseca, B., Hernandez, F., Dengler, M., et al. (2019). The tropical Atlantic observing system. *Frontiers in Marine Science*, 6, 206. <https://doi.org/10.3389/fmars.2019.00206>

Foltz, G. R., & McPhaden, M. J. (2010). Interaction between the Atlantic meridional and Niño modes. *Geophysical Research Letters*, 37(18), L18604. <https://doi.org/10.1029/2010GL044001>

Giannini, A., Saravanan, R., & Chang, P. (2003). Oceanic forcing of Sahel rainfall on interannual to interdecadal time scales. *Science*, 302(5647), 1027–1030. <https://doi.org/10.1126/science.1089357>

Hersbach, H., Bell, B., Berrisford, P., Hirahara, S., Horányi, A., Muñoz-Sabater, J., et al. (2020). The ERA5 global reanalysis. *Quarterly Journal of the Royal Meteorological Society*, 146(730), 1999–2049. <https://doi.org/10.1002/qj.3803>

Hu, S., & Fedorov, A. V. (2019). The extreme El Niño of 2015–2016: The role of westerly and easterly wind bursts, and preconditioning by the failed 2014 event. *Climate Dynamics*, 52(12), 7339–7357. <https://doi.org/10.1007/s00382-017-3531-2>

Jiang, L., Li, T., & Ham, Y. (2022). Asymmetric impacts of El Niño and La Niña on equatorial Atlantic warming. *Journal of Climate*, 36(1), 193–212. <https://doi.org/10.1175/JCLI-D-22-0158.1>

Jin, F. (1997). An equatorial ocean recharge paradigm for ENSO. Part I: Conceptual model. *Journal of the Atmospheric Sciences*, 54(7), 811–829. [https://doi.org/10.1175/1520-0469\(1997\)054<0811:aeorpf>2.0.co;2](https://doi.org/10.1175/1520-0469(1997)054<0811:aeorpf>2.0.co;2)

Kalnay, E., Kanamitsu, M., Kistler, R., Collins, W., Deaven, D., Gandin, L., et al. (1996). The NCEP/NCAR 40-year reanalysis project. *Bulletin of the American Meteorological Society*, 77(3), 437–471. [https://doi.org/10.1175/1520-0477\(1996\)077<0437:tnyrp>2.0.co;2](https://doi.org/10.1175/1520-0477(1996)077<0437:tnyrp>2.0.co;2)

Keenlyside, N. S., & Latif, M. (2007). Understanding equatorial Atlantic interannual variability. *Journal of Climate*, 20(1), 131–142. <https://doi.org/10.1175/jcli3992.1>

Kessler, W. S. (2002). Is ENSO a cycle or a series of events? *Geophysical Research Letters*, 29(23), 2125. <https://doi.org/10.1029/2002GL015924>

Kessler, W. S., McPhaden, M. J., & Weickmann, K. S. (1995). Forcing of intraseasonal Kelvin wave in the equatorial Pacific. *Journal of Geophysical Research*, 100(C6), 10613–10631. <https://doi.org/10.1029/95JC00382>

Kim, D., Lee, S.-K., Lopez, H., Foltz, G. R., Wen, C., West, R., & Dunion, J. (2023). Increase in Cape Verde hurricanes during Atlantic Niño. *Nature Communications*, 14(1), 3704. <https://doi.org/10.1038/s41467-023-39467-5>

Kirtman, B. P., & Schopf, P. S. (1998). Decadal variability in ENSO predictability and prediction. *Journal of Climate*, 11(11), 2804–2822. [https://doi.org/10.1175/1520-0442\(1998\)011<2804:dviapa>2.0.co;2](https://doi.org/10.1175/1520-0442(1998)011<2804:dviapa>2.0.co;2)

Latif, M., & Grötzner, A. (2000). The equatorial Atlantic oscillation and its response to ENSO. *Climate Dynamics*, 16(2–3), 213–218. <https://doi.org/10.1007/s003820050014>

Latif, M., Grötzner, A., & Frey, H. (1996). *El Hermanito: El Niño's overlooked little brother in the Atlantic. (Rep. 196)*. Max-Planck-Institute for Meteorology. Retrieved from [https://pure.mpg.de/rest/items/item\\_3032901\\_1/component/file\\_3032902/content](https://pure.mpg.de/rest/items/item_3032901_1/component/file_3032902/content)

Lee, S.-K., Enfield, D. B., & Wang, C. (2008). Why do some El Niños have no impact on tropical North Atlantic SST? *Geophysical Research Letters*, 35(16), L16705. <https://doi.org/10.1029/2008GL034734>

Lengaigne, M., Guilyardi, E., Boulanger, J.-P., Menkes, C., Delecluse, P., Inness, P., et al. (2004). Triggering of El Niño by westerly wind events in a coupled general circulation model. *Climate Dynamics*, 23(6), 601–620. <https://doi.org/10.1007/s00382-004-0457-2>

Liebmann, B., & Smith, C. A. (1996). Description of a complete (interpolated) outgoing longwave radiation dataset. *Bulletin of the American Meteorological Society*, 77, 1275–1277.

Lopez, H., & Kirtman, B. P. (2015). Tropical Pacific internal atmospheric dynamics and resolution in a coupled GCM. *Climate Dynamics*, 44(1–2), 509–527. <https://doi.org/10.1007/s00382-014-2220-7>

Losada, T., Rodríguez-Fonseca, B., Janicot, S., Gervois, S., Chauvin, F., & Ruti, P. (2010). A multi-model approach to the Atlantic equatorial mode: Impact on the West African monsoon. *Climate Dynamics*, 35(1), 29–43. <https://doi.org/10.1007/s00382-009-0625-5>

Lu, Q., Rao, J., Liang, Z., Guo, D., Luo, J., Liu, S., et al. (2021). The sudden stratospheric warming in January 2021. *Environmental Research Letters*, 16(8), 084029. <https://doi.org/10.1088/1748-9326/ac12f4>

Lübbecke, J. F., & McPhaden, M. J. (2012). On the inconsistent relationship between Pacific and Atlantic Niños. *Journal of Climate*, 25(12), 4294–4303. <https://doi.org/10.1175/jcli-d-11-00553.1>

Lübbecke, J. F., Rodríguez-Fonseca, B., Richter, I., Martín-Rey, M., Losada, T., Polo, I., & Keenlyside, N. S. (2018). Equatorial Atlantic variability-modes, mechanisms, and global teleconnections. *WIREs Climate Change*, 9(4). <https://doi.org/10.1002/wcc.527>

- Luther, D. S., Harrison, D. E., & Knox, R. A. (1983). Zonal winds in the central equatorial Pacific and El Niño. *Science*, 222(4621), 327–330. <https://doi.org/10.1126/science.222.4621.327>
- Martín-Rey, M., & Lazar, A. (2019). Is the boreal spring tropical Atlantic variability a precursor of the Equatorial Mode? *Climate Dynamics*, 53(3–4), 2339–2353. <https://doi.org/10.1007/s00382-019-04851-9>
- Martín-Rey, M., Polo, I., Rodríguez-Fonseca, B., Losada, T., & Lazar, A. (2018). Is there evidence of changes in tropical Atlantic variability modes under AMO phases in the observational record? *Journal of Climate*, 31(2), 515–536. <https://doi.org/10.1175/JCLI-D-16-0459.1>
- Matthews, A. J. (2000). Propagation mechanisms for the Madden-Julian Oscillation. *Quarterly Journal of the Royal Meteorological Society*, 126(569), 2637–2651. <https://doi.org/10.1002/qj.49712656902>
- McPhaden, M. J. (1999). Genesis and evolution of the 1997–1998 El Niño. *Science*, 283(5404), 950–954. <https://doi.org/10.1126/science.283.5404.950>
- McPhaden, M. J. (2004). Evolution of the 2002/03 El Niño. *Bulletin of the American Meteorological Society*, 85(5), 677–696. <https://doi.org/10.1175/BAMS-85-5-677>
- McPhaden, M. J., Freitag, H. P., Hayes, S. P., Taft, B. A., Chen, Z., & Wyrski, K. (1988). The response of the equatorial Pacific Ocean to a westerly wind burst in May 1986. *Journal of Geophysical Research*, 93(C9), 10589–10603. <https://doi.org/10.1029/JC093iC09p10589>
- Meinen, C. S., & McPhaden, M. J. (2000). Observations of warm water volume changes in the equatorial Pacific and their relationship to El Niño and La Niña. *Journal of Climate*, 13(20), 3551–3559. [https://doi.org/10.1175/1520-0442\(2000\)013<3551:oowwvc>2.0.co;2](https://doi.org/10.1175/1520-0442(2000)013<3551:oowwvc>2.0.co;2)
- Okumura, Y., & Xie, S.-P. (2004). Interaction of the Atlantic equatorial cold tongue and the African monsoon. *Journal of Climate*, 17(18), 3589–3602. [https://doi.org/10.1175/1520-0442\(2004\)017<3589:iotaec>2.0.co;2](https://doi.org/10.1175/1520-0442(2004)017<3589:iotaec>2.0.co;2)
- Penland, C., & Sardeshmukh, P. D. (1995). The optimal growth of tropical sea surface temperature anomalies. *Journal of Climate*, 8(8), 1999–2024. [https://doi.org/10.1175/1520-0442\(1995\)008<1999:togots>2.0.co;2](https://doi.org/10.1175/1520-0442(1995)008<1999:togots>2.0.co;2)
- Philander, S. G. H. (1986). Unusual conditions in the tropical Atlantic Ocean in 1984. *Nature*, 322(6076), 236–238. <https://doi.org/10.1038/322236a0>
- Polo, I., Lazar, A., Rodríguez-Fonseca, B., & Arnault, S. (2008). Oceanic Kelvin waves and tropical Atlantic intraseasonal variability: 1. Kelvin wave characterization. *Journal of Geophysical Research*, 113(C7), C07009. <https://doi.org/10.1029/2007JC004495>
- Puy, M., Vialard, J., Lengaigne, M., & Guilyardi, E. (2016). Modulation of equatorial Pacific westerly/easterly wind events by the Madden–Julian oscillation and convectively-coupled Rossby waves. *Climate Dynamics*, 46(7–8), 2155–2178. <https://doi.org/10.1007/s00382-015-2695-x>
- Puy, M., Vialard, J., Lengaigne, M., Guilyardi, E., DiNezio, P. N., Voltaire, A., et al. (2019). Influence of westerly wind events stochasticity on El Niño amplitude: The case of 2014 vs. 2015. *Climate Dynamics*, 52(12), 7435–7454. <https://doi.org/10.1007/s00382-017-3938-9>
- Rayner, N. A., Parker, D. E., Horton, E. B., Folland, C. K., Alexander, L. V., Rowell, D. P., et al. (2003). Global analyses of sea surface temperature, sea ice, and night marine air temperature since the late nineteenth century. *Journal of Geophysical Research*, 108(D14), 4407. <https://doi.org/10.1029/2002JD002670>
- Richter, I., Tokinaga, H., & Okumura, Y. M. (2022). The extraordinary equatorial Atlantic warming in late 2019. *Geophysical Research Letters*, 49(4), e2021GL095918. <https://doi.org/10.1029/2021GL095918>
- Schouten, M. W., Matano, R. P., & Strub, T. P. (2005). A description of the seasonal cycle of the equatorial Atlantic from altimeter data. *Deep Sea Research Part I: Oceanographic Research Papers*, 52(3), 477–493. <https://doi.org/10.1016/j.dsr.2004.10.007>
- Suarez, M. J., & Schopf, P. S. (1988). A delayed action oscillator for ENSO. *Journal of the Atmospheric Sciences*, 45(21), 3283–3287. [https://doi.org/10.1175/1520-0469\(1988\)045<3283:adaofe>2.0.co;2](https://doi.org/10.1175/1520-0469(1988)045<3283:adaofe>2.0.co;2)
- Timmermann, A., An, S.-I., Kug, J.-S., Jin, F.-F., Cai, W., Capotondi, A., et al. (2018). El Niño–Southern Oscillation complexity. *Nature*, 559(7715), 535–545. <https://doi.org/10.1038/s41586-018-0252-6>
- Tokinaga, H., Richter, I., & Kosaka, Y. (2019). ENSO influence on the Atlantic Niño, revisited: Multi-year versus single-year ENSO events. *Journal of Climate*, 32(14), 4585–4600. <https://doi.org/10.1175/JCLI-D-18-0683.1>
- Tschakert, P., Sagoe, R., Ofori-Darko, G., & Codjoe, S. N. (2010). Floods in the Sahel: An analysis of anomalies, memory and anticipatory learning. *Climatic Change*, 103(3–4), 471–502. <https://doi.org/10.1007/s10584-009-9776-y>
- Vallès-Casanova, I., Lee, S.-K., Foltz, G. R., & Pelegrí, J. L. (2020). On the spatiotemporal diversity of Atlantic Niño and associated rainfall variability over West Africa and South America. *Geophysical Research Letters*, 47(8), e2020GL087108. <https://doi.org/10.1029/2020GL087108>
- van Oldenborgh, G. J. (2000). What caused the onset of the 1997–98 El Niño? *Monthly Weather Review*, 128(7), 2601–2607. [https://doi.org/10.1175/1520-0493\(2000\)128<2601:wctoot>2.0.co;2](https://doi.org/10.1175/1520-0493(2000)128<2601:wctoot>2.0.co;2)
- Vecchi, G. A., & Harrison, D. E. (2000). Tropical Pacific sea surface temperature anomalies, El Niño, and equatorial westerly wind events. *Journal of Climate*, 13(11), 1814–1830. [https://doi.org/10.1175/1520-0442\(2000\)013<1814:tpssta>2.0.co;2](https://doi.org/10.1175/1520-0442(2000)013<1814:tpssta>2.0.co;2)
- Vecchi, G. A., Wittenberg, A. T., & Rosati, A. (2006). Reassessing the role of stochastic forcing in the 1997–1998 El Niño. *Geophysical Research Letters*, 33(1), L01706. <https://doi.org/10.1029/2005GL024738>
- Wang, H., & Fu, R. (2007). The influence of Amazon rainfall on the Atlantic ITCZ through convectively coupled Kelvin waves. *Journal of Climate*, 20(7), 1188–1201. <https://doi.org/10.1175/jcli4061.1>
- Wheeler, M. C., & Hendon, H. H. (2004). An all-season real-time multivariate MJO index: Development of an index for monitoring and prediction. *Monthly Weather Review*, 132(8), 1917–1932. [https://doi.org/10.1175/1520-0493\(2004\)132<1917:aarmmi>2.0.co;2](https://doi.org/10.1175/1520-0493(2004)132<1917:aarmmi>2.0.co;2)
- Wyrski, K. (1985). Water displacements in the Pacific and the genesis of El Niño cycles. *Journal of Geophysical Research*, 90(C4), 7129–7132. <https://doi.org/10.1029/JC090iC04p07129>
- Yu, W., Han, W., Maloney, E. D., Gochis, D., & Xie, S.-P. (2011). Observations of eastward propagation of atmospheric intraseasonal oscillations from the Pacific to the Atlantic. *Journal of Geophysical Research*, 116(D2), D02101. <https://doi.org/10.1029/2010JD014336>
- Zebiak, S. E. (1993). Air–sea interaction in the equatorial Atlantic region. *Journal of Climate*, 6(8), 1567–1586. [https://doi.org/10.1175/1520-0442\(1993\)006<1567:aiitea>2.0.co;2](https://doi.org/10.1175/1520-0442(1993)006<1567:aiitea>2.0.co;2)
- Zhang, C., & Gottschalck, J. (2002). SST anomalies of ENSO and the Madden-Julian Oscillation in the equatorial Pacific. *Journal of Climate*, 15(17), 2429–2445. [https://doi.org/10.1175/1520-0442\(2002\)015<2429:saoeat>2.0.co;2](https://doi.org/10.1175/1520-0442(2002)015<2429:saoeat>2.0.co;2)
- Zhao, S., & Fu, R. (2022). The influence of convectively coupled Kelvin waves on Atlantic Niños. *Journal of Geophysical Research: Atmospheres*, 127(9), e2021JD036241. <https://doi.org/10.1029/2021JD036241>
- Zuo, H., Balmaseda, M. A., & Mogensen, K. (2017). The new eddy-permitting ORAP5 ocean reanalysis: Description, evaluation and uncertainties in climate signals. *Climate Dynamics*, 49(3), 791–811. <https://doi.org/10.1007/s00382-015-2675-1>